HOSTED BY

ELSEVIER

CrossMark

Available online at www.sciencedirect.com

ScienceDirect

Defence Technology 11 (2015) 220–228

www.elsevier.com/locate/dt

Effect of hot-humid exposure on static strength of adhesive-bonded aluminum alloys

Rui ZHENG [a], Jian-ping LIN [a,*], Pei-Chung WANG [b], Yong-Rong WU [a]

[a] School of Mechanical Engineering, Tongji University, Shanghai 201804, China

[b] Global Research & Development Center, General Motors Corporation, Warren, MI 48090-9055, USA

Received 30 November 2014; revised 31 December 2014; accepted 19 January 2015

Available online 10 April 2015

Abstract

The effect of hot-humid exposure (i.e., 40 °C and 98% R.H.) on the quasi-static strength of the adhesive-bonded aluminum alloys was studied. Test results show that the hot-humid exposure leads to the significant decrease in the joint strength and the change of the failure mode from a mixed cohesive and adhesive failure with cohesive failure being dominant to adhesive failure being dominant. Careful analyses of the results reveal that the physical bond is likely responsible for the bond adhesion between ***L*** adhesive and aluminum substrates. The reduction in joint strength and the change of the failure mode resulted from the degradation in bond adhesion, which was primarily attributed to the corrosion of aluminum substrate. In addition, the elevated temperature exposure significantly accelerated the corrosion reaction of aluminum, which accelerated the degradation in joint strength.

Keywords: Epoxide adhesive; Aluminum alloy; Hot-humid exposure; Static strength; Bond adhesion

1. Introduction

The use of adhesive is posed to increase dramatically for application to the next generation of vehicle structures as the use of lightweight materials (e.g., aluminum and magnesium alloys) [1–3]. In spite of this, the use of adhesive-bonded aluminum joints in vehicle structures has been limited, mainly due to the degradation of crashworthiness and structural durability caused by the hot-humid exposure [4,5].

In vehicle structures, the majority of the adhesive-bonded components is exposed to the environment of temperature and moist air. Previous studies revealed that if the exposure was over a significant period of time, the joint strength gradually declined [6] which was closely related to the water absorption of the adhesive-bonded joints [7,8]. Many studies [9–12] on effect of hot-humid exposure on the strength of the adhesive-bonded aluminum alloys showed that the hot-humid exposure significantly decreased the strengths of the adhesive-bonded aluminum joints. The strength degradation primarily resulted from that water absorption in the interface between adhesive and adherend, which resulted in the surface electrochemical corrosion of aluminum adherend, and consequently led to the degradation in the interfacial bond between adhesive and adherend. To improve the corrosion resistance of the adhesive-bonded aluminum joints, various surface treatments of aluminum were utilized. Lunder et al. [10] investigated the effect of surface pretreatment of aluminum alloys on the joint strength and found that the improvement in corrosion resistance of treated aluminum alloys significantly promoted the durability of the bonded joints. However, although these surface pretreatments improved the corrosion resistance of aluminum, there was still a slight decrease in joint strength,

* Corresponding author. Tel.: +86 139 0171 9457; fax: +86 021 6958 9485.
E-mail address: jplin58@tongji.edu.cn (J.P. LIN).

Peer review under responsibility of China Ordnance Society.

http://dx.doi.org/10.1016/j.dt.2015.01.005

Table 1
Chemical composition (Wt. %) of Novelis X610-T4PD (X1.0) and X626-T4P (X0.9) aluminum alloys.

Substrate	Mg/%	Si/%	S/%	Ti/%	Mn/%	Al/%
X1.0	0.63	0.82	0.01	0.05	0.12	Balance
X0.9	0.46	1.14	0.01	0.02	0.12	Balance

and the treated aluminum in the overlap region was not corroded by the electrochemical reaction. Furthermore, the degradation mechanism of the adhesive-bonded aluminum alloys exposed to hot-humid environment has been still unclear.

In the present study, the effect of hot-humid exposure on the strength of the adhesive-bonded aluminum joints is investigated. The strength of the adhesive-bonded aluminum joint is evaluated using lap-shear joint configuration. Differential scanning calorimetry (DSC), contact angle measurement, surface free energy dispersive X-ray spectroscopy (EDS) and polarization corrosion test are utilized to analyze the degradation mechanism of adhesive-bonded aluminum joints exposed to hot-humid environment. Finally, the effect of elevated temperature in hot-humid environment on the corrosion resistance of the adhesive-bonded aluminum joints is discussed.

2. Experimental

2.1. Materials

1.0 mm thick bare Novelis X610-T4PD (hereafter referred to as **X1.0**) and 0.9 mm thick bare Novelis X626-T4P (hereafter referred to as **X0.9**) aluminum alloys (hereafter referred to as XX substrates) were used in this study. ***L*** adhesive (i.e., a bi-component epoxy-modified acrylic adhesive containing 0.25 mm diameter glass beads to control the bondline thickness) was selected to bond XX aluminum substrates. The main chemical composition of aluminum substrates were measured by X-ray fluorescence spectroscopy (Bruker AXS SRS 3400, Germany), referring to Table 1. The mechanical properties of aluminum substrates provided by supplier are listed in Table 2. Table 3 lists the mechanical properties of ***L*** adhesive provided by supplier.

2.2. Sample fabrication

All substrates were sheared into 25 mm × 100 mm samples which were cleaned by 1-1-1 trichloroethane. ***L*** adhesive was applied to the substrates, and the top sheet was set down upon the bottom sheet per the lap-shear joint configuration (hereafter referred to as XXL joint), as shown in Fig. 1. The adhesive-bonded samples were prepared as follows: (a) applying the adhesive on one of the two adherends using a hand-held injection gun, and positioning the adherends with and without dispensed adhesive using a fixture; (b) bringing the adherends together by a fixture under ambient laboratory conditions, and a pressure was applied via the fixture so that a bondline thickness of 0.25 mm can be maintained; (c) curing the samples in the oven as per the supplier's recommended curing procedure (i.e., 16 h at room temperature and then 20 min at 170 °C). The schematic diagram of adhesive bonding process for aluminum alloys is presented in Fig. 2. All finished samples were examined and the spew fillets around the edge of the overlap were retained to simulate real production conditions.

Table 2
Mechanical properties of Novelis X610-T4PD (X1.0) and X626-T4P (X0.9) aluminum alloys.

Substrate	Yield strength/MPa	Ultimate tensile strength/MPa	Total elongation/%
X1.0	119.9	228.6	21.9
X0.9	108.7	214.8	22.4

Table 3
Mechanical properties of *L* adhesive.

Material	Yield strength/MPa	Tensile strength/MPa	Elongation/%
L adhesive	3.7	8.9	28.6

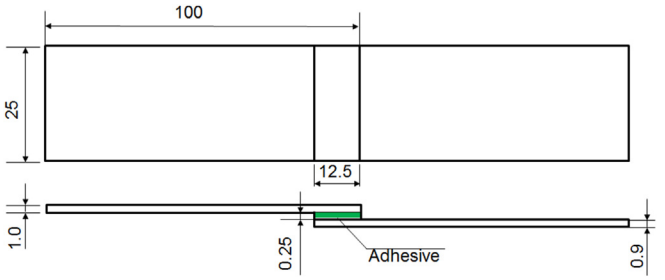

Fig. 1. Configuration of adhesive-bonded lap-shear joint (dimensions in mm).

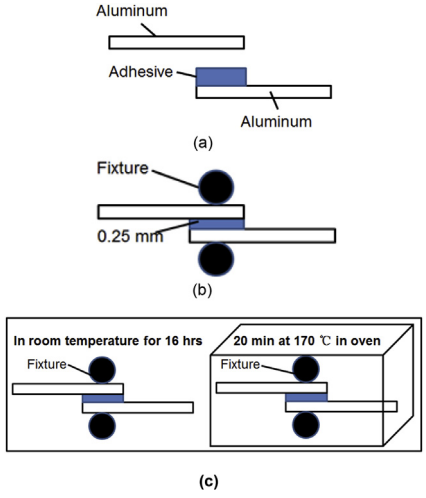

Fig. 2. Schematic diagram of adhesive bonding process for aluminum alloys (a) Applying adhesive and positioning the aluminum substrates (b) Pressure is applied by the fixture to maintain a bondline thickness of 0.25 mm (c) Curing the samples for 16 h at room temperature and then 20 min at 170 °C.

2.3. Differential scanning calorimetry

Differential scanning calorimetry (DSC) has been extensively used to investigate the chemical reaction process [13,14]. In this study, DSC measurement was performed for ***L*** adhesive to know the change in the exothermic enthalpy of adhesive using TA Instruments DSC Q100 [15]. For the DSC measurement of adhesive, the adhesive with a weight of 20–25 mg was placed in a hermetic crucible, and an equivalent pan was used as a reference. Also, the adhesive with similar weight (about 20–25 mg) was placed in a hermetic crucible with aluminum substrate (i.e., bare Novelis X610-T4PD (**X1.0**) or X626-T4P (**X0.9**), aluminum substrate was cut into round to be firstly filled into a crucible), and an equivalent pan with aluminum substrate was uses as a reference. Quantitative dynamic scans ramped at 15 °C/min from 0 °C to 200 °C with a heating rate being approximately equivalent to the rate for the lap-shear joints in curing process.

2.4. Contact angle measurement and surface free energy

Good wettability of a surface is a prerequisite for good adhesion [16]. Contact angle is closely related to wettability. For the purpose of investigating the effect on the strength and failure mode of the adhesive-bonded joint, the surface free energy of the substrates was estimated by measuring the contact angle of test liquids on the substrates. Distilled water, diiodomethane and ethylene glycol were used as a probe to measure the contact angle of the aluminum substrates by the sessile drop method with a Dataphysics OCA-20 contact angle analyzer [17] at 23 °C. The volume of a test drop is 2 μL. The liquids were chosen to cover the broadest possible range from highly polar (water) to almost completely dispersion (diiodomethane). The data of the surface tension and surface tension components of test liquids at 23 °C are given in Table 4 [18].

This measurement method is based on Young's equation [19], which describes the condition for equilibrium at a solid–liquid interface.

$$\gamma_L \cos\theta = \gamma_S - \gamma_{SL} \tag{1}$$

where γ_L is the experimentally determined surface tension of liquid, θ is the contact angle, γ_S is the surface free energy of the solid, and γ_{SL} is the solid–liquid interfacial energy.

In order to obtain the solid surface free energy, γ_S, an estimate of γ_{SL}, must be obtained. Owens et al. [20] extended Fowkes's ideas [21] and proposed a geometric mean approach to combine the dispersion and non-dispersion (polar) interactions, and the following expression for γ_{SL} was applied

$$\gamma_{SL} = \gamma_S + \gamma_L - 2\sqrt{\gamma_S^d \gamma_L^d} - 2\sqrt{\gamma_S^p \gamma_L^p} \tag{2}$$

Combining Eq. (2) with Eq. (1) yields

$$\gamma_L(1+\cos\theta) = 2\sqrt{\gamma_S^d \gamma_L^d} + 2\sqrt{\gamma_S^p \gamma_L^p} \tag{3}$$

The contact angle of at least two liquids with known surface tension components (γ_L;γ_L^d;γ_L^p) on the solid must be determined to obtain γ_S^d and γ_S^p of a measured material. In this case, three liquids (i.e., distilled water, diiodomethane and ethylene glycol) were used to determine γ_S^d and γ_S^p of these aluminum substrates.

Bond adhesion between adhesive and substrate is a key for sound joint strength [16], which is related to the work of adhesion. In order to assess the bond adhesion between adhesive and substrate, the work of adhesion was calculated with Dupre equation [22].

$$W_{Ad} = \gamma_S + \gamma_L - \gamma_{SL} \tag{4}$$

where the energy of bond adhesion (W_{Ad}) is directly related to the surface free energy of the two adjacent phases ***S*** (substrates) and ***L*** (adhesive). Combining Eqs. (2) and (4), we have

$$W_{Ad} = 2\sqrt{\gamma_S^d \gamma_L^d} + 2\sqrt{\gamma_S^p \gamma_L^p} \tag{5}$$

2.5. Hot-humid exposure

To simulate the extended exposure in corrosion environment, the bonded joints were exposed to 98% relatively humidity and 40 °C for 240 h. The joints were removed from the hot-humid chamber shown in Fig. 3 and immediately quasi-static tested.

Table 4
Test liquids and their surface tension components [18].

Liquids	Temperature/°C	Surface tension data/(mN·m^{-1})		
		γ_L	γ_L^d	γ_L^p
Distilled water	23	72.8	21.8	51.0
Diiodomethane	23	50.8	50.8	0
Ethylene glycol	23	48	29	19.0

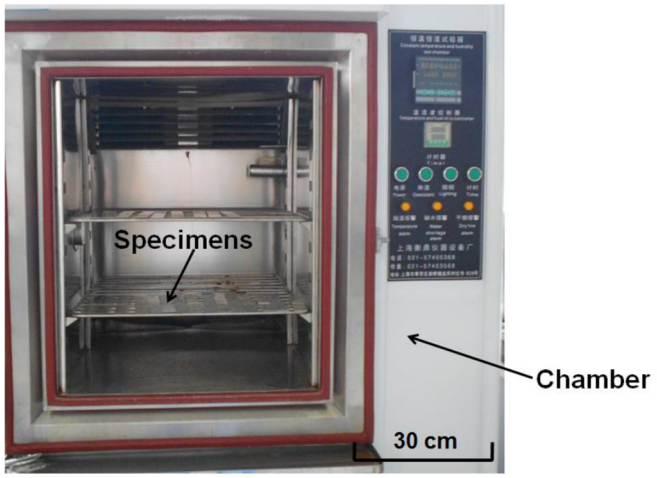

Fig. 3. Samples exposed to the hot-humid testing chamber.

2.6. Quasi-static testing

The cured samples were kept at room temperature for 24 h, and then the quasi-static test was performed by loading each sample to failure in Zwick Z050 tensile tester according to the standard ASTM D1002-2001 [23] for the determination of the joint strength. To minimize the bending stresses inherent in the testing of single-lap shear samples, filler plates i.e. shims, were attached to both ends of the sample using masking tape to accommodate the sample offset. Load vs. displacement curves were obtained as the samples were loaded at a stroke rate of 10 mm/min. The joint strength is evaluated by using the peak load. Five replicates were performed, and the average peak loads were reported.

2.7. Fractography

Post-failure analysis was performed with an optical microscope to study the failure mechanisms for both as-fabricated and neutral salt spray exposure samples. Fractography samples were cut from the surface of fractured overlap sections.

2.8. Corrosion resistance

The polarization curves [24] of aluminum substrates in 3.5% NaCl solution at 23 °C and 40 °C, respectively, were measured to evaluate the corrosion resistance of the X610-T4PD and X626-T4P aluminum. A saturated calomel electrode was used as a reference electrode, and a large-area Pt electrode was used as the assistant electrode. A sample area of 3.125 cm^2 was exposed to the solution and the scanning speed was 0.8 mV/s.

3. Results and discussion

3.1. Effect of hot-humid exposure on joint strength

Lap-shear joints were fabricated and exposed under hot-humid conditions (i.e., 98% R.H. and 40 °C) for 240 h, and then removed for quasi-static testing. Fig. 4 presents the effect of hot-humid exposure on the strength of adhesive-bonded lap X610-T4PD and X626-T4P aluminum joints. As shown, the hot-humid exposure decreased significantly the strength of the adhesive-bonded joints. To understand the decrease in joint strength, the fractography of the tested adhesive-bonded joints was observed in Fig. 5. It can be seen that the hot-humid exposure changed the failure mode from a mixed cohesive and adhesive failure with cohesive failure being dominant to adhesive failure being dominant.

The significant degradation in joint strength of the exposed adhesive-bonded aluminum may be attributed to the decline of the inherent mechanical properties of ***L*** adhesive and the reduction in bond adhesion between the adhesive and substrate or a combination of the two. To understand the cause of the strength reduction, the effect of hot-humid exposure on the properties of ***L*** adhesive and the bond adhesion between adhesive and aluminum was investigated and will be described next.

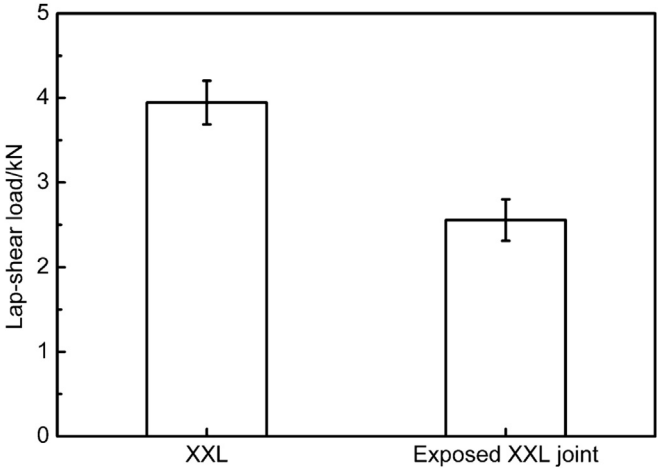

Fig. 4. Effect of hot-humid exposure on strength of adhesive-bonded 1.0 mm thick X610T4PD and 0.9 mm thick X626-T4P aluminum joints.

3.2. Effect of hot-humid exposure on properties of L adhesive

In order to understand the effect of hot-humid exposure on the mechanical properties of ***L*** adhesive, ***L*** adhesive was carefully removed from the exposed samples and immediately analyzed by differential scanning calorimetry (DSC). Fig. 6 shows the effect of a hot humid exposure on the thermograms of unexposed and exposed ***L*** adhesive samples. As shown, the hot-humid exposure had little influence on the curing extent and glass transition temperature (~40 °C) of ***L*** adhesive, which means that the adhesive properties were degraded little by the environmental exposure. Therefore, in terms of degrading the joint strength, the adhesive degradation resulting from hot humid exposure was ruled out. These results

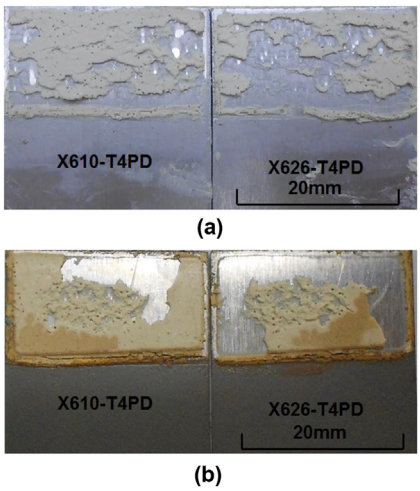

Fig. 5. Effect of hot-humid exposure on fractography of adhesive-bonded 1.0 mm thick X610-T4PD and 0.9 mm thick X626-T4P aluminum joints (a) As-fabricated (b) Exposed to hot-humid conditions (i.e., 98% R.H. and 40 °C).

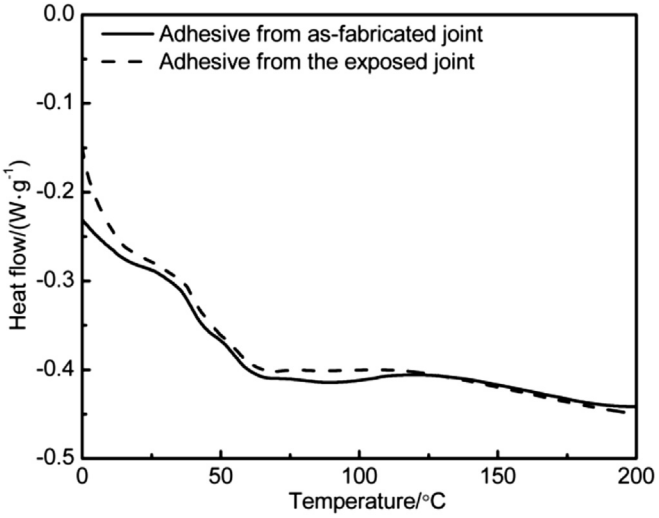

Fig. 6. Effect of hot-humid exposure (i.e., 40 °C and 98% R.H. for 10 days) on the thermograms of ***L*** adhesive from adhesive-bonded 1.0 mm thick X610-T4PD and 0.9 mm thick X626-T4P joints.

indicate that the reduction in joint strength is likely caused by the degradation in bond adhesion between adhesive and aluminum substrates. Liu et al. [25] also found similar results by studying the effect of hot-humid exposure on the durability of adhesive-bonded magnesium AZ31.

3.3. Adhesion characteristic between adhesive and aluminum

Adhesion is the interatomic and intermolecular interaction at the interface of two surfaces [26]. It is well known that the physical or chemical bonds are primarily responsible for the adhesion between adhesive and adherend [16,27]. In order to identify if the existence of chemical bonds between the adhesive and aluminum adherends of the adhesive-bonded XXL joint, DSC tests of the adhesive and adhesive with aluminum samples were conducted. As a result of the process of forming new chemical bonds accompanied by the heat release, it may induce the exothermic difference between the adhesive and adhesive on the aluminum adherend samples in the curing process. Uncured ***L*** adhesive samples positioned in a crucible with a bare aluminum substrate and on bare aluminum coupons were tested and the representative results are presented in Fig. 7. As shown in Fig. 7, the DSC results for ***L*** adhesive-in-crucible, ***L*** adhesive-on-Novelis X610-T4PD and ***L*** adhesive-on-Novelis X626-T4P samples in a crucible exhibited little

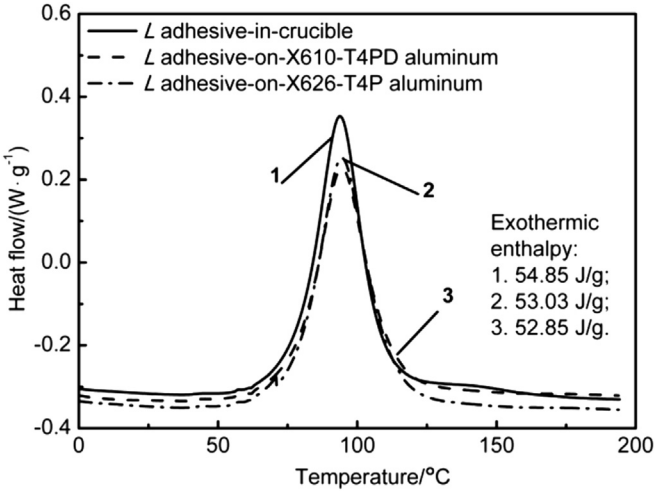

Fig. 7. Thermograms of ***L*** adhesive with and without 1.0 mm thick X610-T4PD and 0.9 mm thick X626-T4P aluminum at a rate of 15 °C/min.

difference except for the difference in heat flow. The careful examination of DSC analysis results revealed that the difference in exothermic enthalpy (i.e., integral of heat flow and peak area shown in curves 1, 2 and 3 in Fig. 7) was likely caused by the difference in sample weight. These results suggested that little chemical reaction was occurred in the heating process between ***L*** adhesive and bare Novelis X610-T4PD and Novelis X626-T4P aluminum. In other words, the physical bond was likely responsible for the bond adhesion between ***L*** adhesive and aluminum substrates.

To assess the bond adhesion between adhesive and aluminum adherend, the work of adhesion between adhesive and aluminum adherend was estimated. As indicated in Eq. (5), to estimate the work of adhesion between adhesive and aluminum adherend, the surface free energies and their components of adhesive and aluminum were firstly estimated by the measured contact angles of three testing liquids (i.e., distilled water, ethylene glycol, and diiodomethane) upon the adhesive and aluminum adherends.

Table 5 lists the contact angles of these test liquids upon the aluminum adherends. In addition, the contact angles of ***L*** adhesive were measured by dispensing them on a substrate. The measurements were immediately performed as soon as the adhesive was dispensed on the adherends. The results are listed in Table 6.

The surface free energies of XX aluminum adherends were estimated based on the method in Ref. [20] and the results are graphically presented in Fig. 8. As shown, the surface free

Table 5
Contact angles of X610-T4PD and X626-T4P aluminum adherends.

Adherends	Distilled water		Ethylene glycol		Diiodomethane	
	Contact angle /(°)	Standard deviation /(°)	Contact angle /(°)	Standard deviation /(°)	Contact angle /(°)	Standard deviation /(°)
X610-T4PD	94.3	1.93	79.3	0.74	56.7	1.05
X626-T4P	93.4	1.01	70.9	0.35	54.8	1.20

Table 6
Contact angles of ***L*** adhesive.

Adhesive	Distilled water		Ethylene glycol		Diiodomethane	
	Contact angle /(°)	Standard deviation /(°)	Contact angle /(°)	Standard deviation /(°)	Contact angle /(°)	Standard deviation /(°)
L	55.9	3.20	45.8	0.50	56.6	2.05

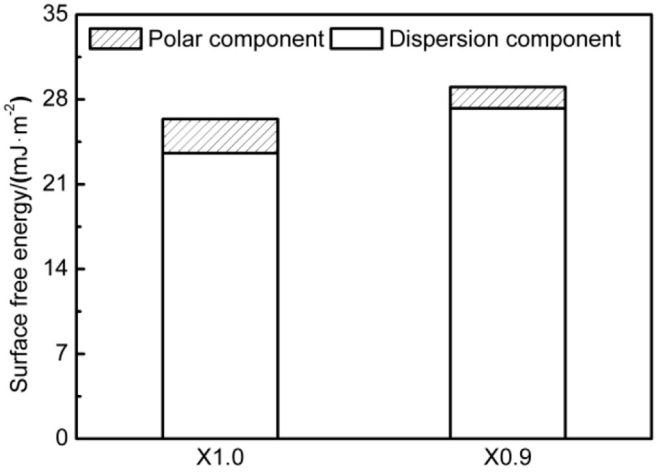

Fig. 8. Calculated surface free energy of as-received 1.0 mm thick X610-T4PD and 0.9 mm thick X626-T4P aluminum adherends.

energy of X610-T4PD aluminum was comparable to that of X626-T4P aluminum. The surface free energy of ***L*** adhesive was estimated, and its dispersion and polar components were 22.25 and 22.02 mJ/m^2, respectively.

Based on Eq. (5), the work of adhesion between X610-T4P and X626-T4P aluminum adherends and ***L*** adhesive was estimated and the results are presented in Fig. 9. As shown, the work of adhesion between X626-T4P aluminum adherend and ***L*** adhesive was comparable to that between X610-T4P aluminum adherend and ***L*** adhesive. Therefore, it can be deduced that the bond strengths between the adhesive and X610-T4PD aluminum were similar to that of X626-T4P aluminum.

3.4. Degradation mechanisms

The decrease in joint strength was likely attributed to the degradation of intermolecular physical bond between adhesive and aluminum. To understand the degradation in strength of the exposed adhesive-bonded joints, the effect of hot-humid exposure on the physical adhesion between adhesive and aluminum is discussed next.

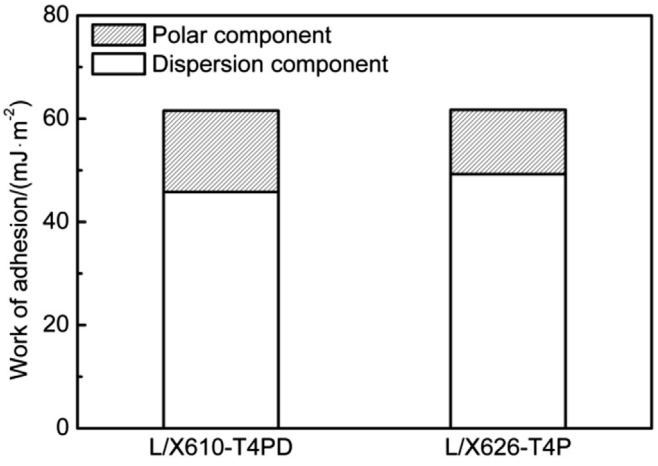

Fig. 9. Calculated work of adhesion between ***L*** adhesive and aluminum adherends in adhesive-bonded 1.0 mm thick X610-T4PD and 0.9 mm thick X626-T4P joints.

The work of adhesion of the bonded aluminum joint consists of intermolecular van del Waals force (i.e., all intermolecular dispersion force, polar or polar-nonpolar intermolecular orientation force and polar-nonpolar intermolecular induction force) and hydrogen bonds [28] which relates directly to the polar component W_p and dispersion component W_d of the work of adhesion. When the adhesive-bonded aluminum joint was exposed to hot-humid conditions, the strong polar water molecules primarily destroyed the hydrogen bond and dissolved many polar molecules [12,29] to decrease the polar component, W_p, and slightly degraded the dispersion component, W_d, of the work of adhesion in the interface of the adhesive-bond joint, which would weaken the joint strength without electrochemical reaction. Furthermore, water molecular may diffuse into the interface between adhesive and substrate [30], which may lead to the electrochemical reaction of aluminum substrate in the overlap of the adhesive-bonded joint. The electrochemical reaction equations governing the corrosion of the aluminum substrate are:

$$Al \rightarrow Al^{3+} + 3e^- \quad (6)$$

$$O_2 + 2H_2O + 4e^- \rightarrow 4OH^- \quad (7)$$

$$2H^+ + 2e^- \rightarrow H_2\uparrow \quad (8)$$

To study if the existence of electrochemical reaction for the aluminum exposed to the hot-humid condition (i.e., 98% R.H. and 40 °C), the oxygen contents of the as-received X610-T4PD aluminum substrate and aluminum substrate on the fracture surfaces from the hot-humid exposed adhesive-bonded joint were examined by energy dispersive spectrometer (EDS). The results are shown in Fig. 10. As shown, the hot-humid exposure increased the oxygen content of aluminum, which suggests that the aluminum substrate on the fracture surfaces from the exposed joints was corroded under the hot-humid conditions. Similar results were also observed by Vera et al. [31]. The electrochemical reaction changed the surface chemistry and structure of aluminum substrate in the overlap region, and consequently resulted in a degradation in intermolecular force [32] at the interface between adhesive and aluminum substrate, which reduced the dispersion component, W_d, and polar component, W_p, of the work of adhesion. In other words, the degradation in bond adhesion between adhesive and aluminum was ascribed to the corrosion of aluminum and the polar component of work of adhesion between adhesive and aluminum being destroyed by moisture, which the corrosion of aluminum was dominant.

In addition, temperature had a significant influence on the chemical reaction of aluminum [33]. To understand the effect of temperature in the hot-humid condition on the strength of the adhesive-bonded joint, the corrosion tests of exposed adhesive-bonded aluminum joints were performed.

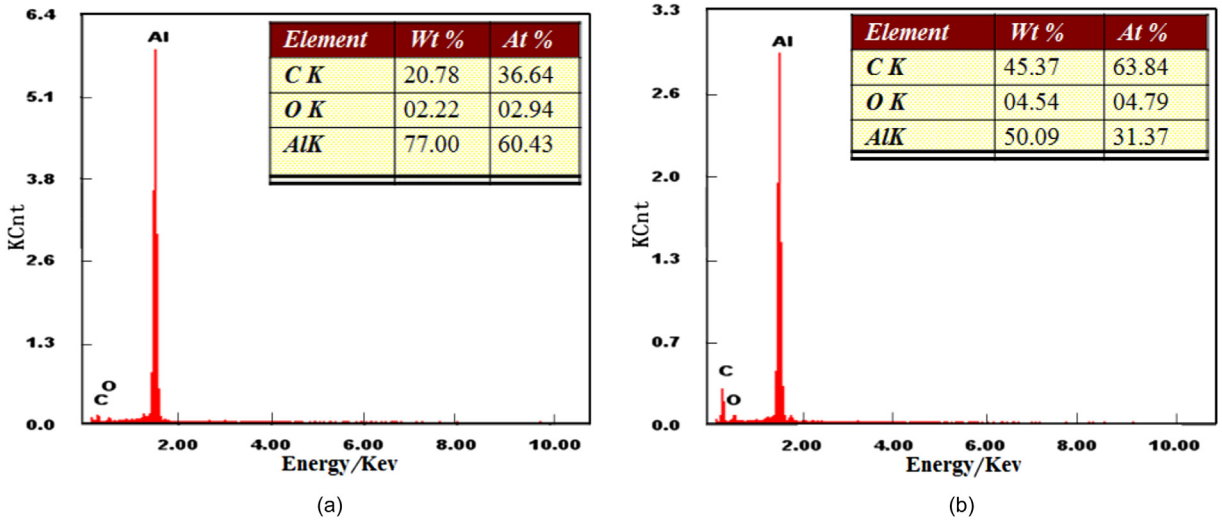

(a) (b)

Fig. 10. Oxygen content of 1.0 mm thick Novelis X610-T4PD (a) As-received (b) On the exposed fracture surfaces.

3.5. Effect of temperature on corrosion resistance of aluminum substrates

To understand the effect of temperature on the corrosion resistance of aluminum substrates, the polarization curves of X610-T4PD and X626-T4P aluminum substrates immersed in 3.5% NaCl solution at 23 °C and 40 °C were measured. The measured results are shown in Fig. 11. As shown in Fig. 11(a), while pitting corrosion occurred in the polarization process of aluminum substrate X610-T4PD at 23 °C, little pitting corrosion (i.e., a smooth curve) was observed for the anodic curve at 40 °C. Furthermore, it can be seen from the polarization curves that the elevated temperature (i.e., 40 °C) accelerates the corrosion of aluminum. For X626-T4P aluminum shown in Fig. 11(b), although the temperature slightly decreased the self-corrosion current, the corrosion current rapidly increased after the passivation film of X626-T4P aluminum was generated. These results suggest that the temperature accelerates the corrosion of X626-T4P aluminum. Therefore, it can be deduced that the temperature likely increases the corrosion resistance of aluminum substrates, and consequently speeds up the degradation in joint strength. To validate this, the joints were exposed to 98% R.H. at 23 °C and 40 °C for 240 h and then tested. The results are presented in Fig. 12. As shown, the decrease in strength of the adhesive-bonded joint exposed to 98% R.H. at 23 °C was smaller than that exposed to 98% R.H. at 40 °C. Furthermore, the areas of adhesive failure of the adhesive-bonded joint exposed to 98% R.H. at 23 °C and 40 °C were examined and shown in Fig. 13. It can be seen from Fig. 13 that the degree of adhesive failure (i.e., 79.1%) of the joints exposed to 98% R.H. at 40 °C was significantly greater than that exposed to 98% R.H. at 23 °C (i.e., 55.3%), which reveals that the temperature of 40 °C under the hot-humid condition (i.e., 98% R.H. and 40 °C) leads to a more serious degradation in failure mode. These results suggest that the elevated temperature (i.e., 40 °C) speeds up the degradation in strength and failure modes of the adhesive-bonded aluminum joints.

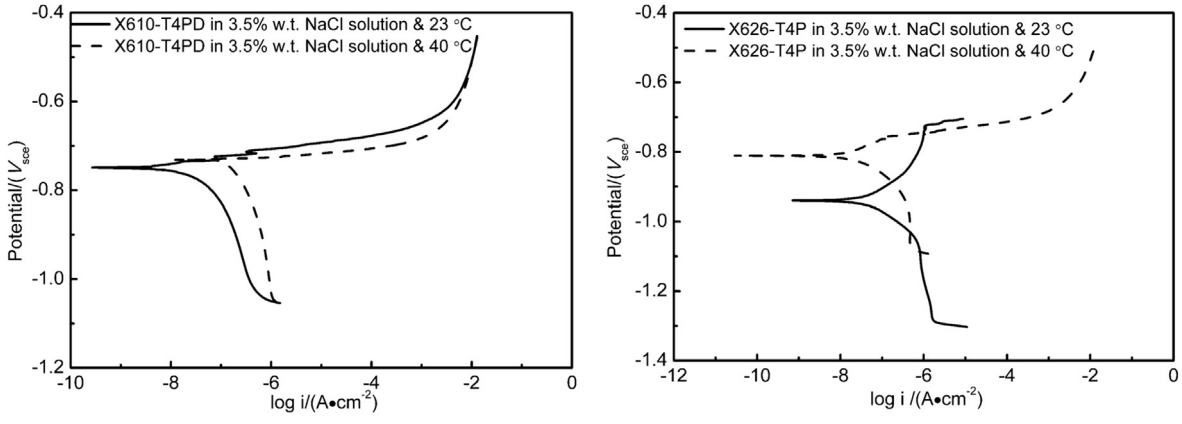

(a) (b)

Fig. 11. Effect of temperature on the polarization curves (a) 1.0 mm thick X610-T4PD (b) 0.9 mm thick X626-T4P aluminum substrates.

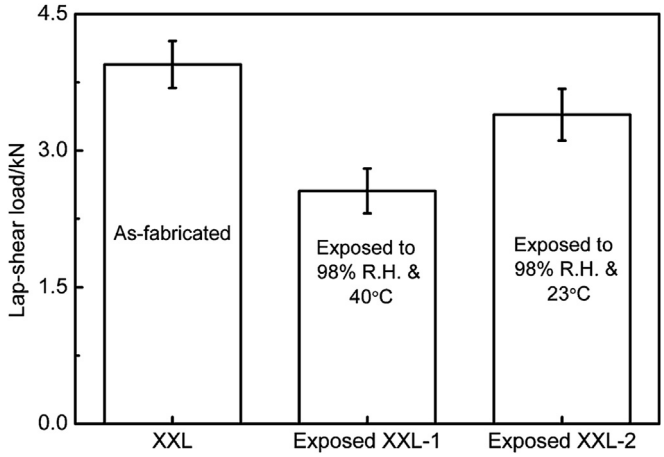

Fig. 12. Effect of hot-humid exposure on the retained strengths of adhesive-bonded aluminum.

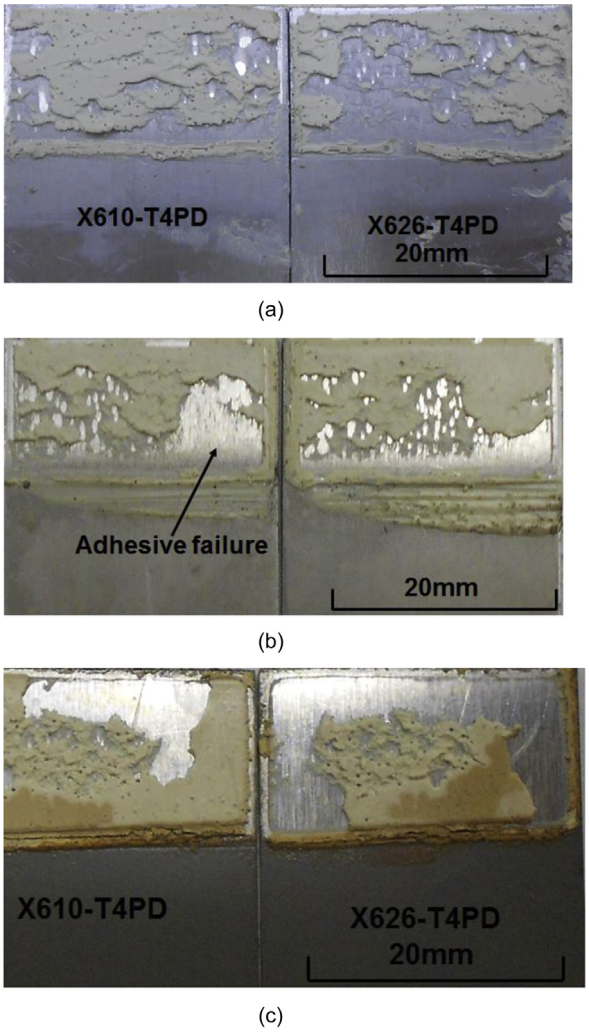

Fig. 13. Effect of temperature on the fractography of adhesive-bonded aluminum jointsjoints (a) Without any exposure and exposed to 98% R. H (b) At 23 °C (c) At 40 °C.

4. Conclusions

Experiments were conducted to characterize the effect of hot-humid exposure on the quasi-static strength of adhesive-bonded lap-shear 1.0 mm thick X610-T4PD and 0.9 mm thick X626-T4P aluminum joints. The following conclusions are achieved:

1) Hot-humid exposure (i.e., 40 °C and 98% R.H. for 240 h) significantly decreased the joint strength and changed the failure mode from a mixed cohesive and adhesive with cohesive failure being dominant to adhesive failure being dominant.
2) The degradation in joint strength and failure mode were primarily attributed to the polar component of work of adhesion between adhesive and aluminum being destroyed by moisture and corrosion of aluminum substrate in the overlap region of the bonded joints, which degraded both polar and dispersion components of work of adhesion between adhesive and aluminum substrate.
3) The elevated temperature significantly accelerated the corrosion reaction of aluminum, which speeds up the degradation in joint strength.

Acknowledgments

This work was funded by General Motors Global Research and Development Center (Grant No.: PS21025708). The authors gratefully acknowledge Robert Szymanski for material preparation and handling.

References

[1] Kahraman R, Sunar M, Yilbas B. Influence of adhesive thickness and filler content on the mechanical performance of aluminum single-lap joints bonded with aluminum powder filled epoxy adhesive. J Mater Process Technol 2008;205:183–9.
[2] Zheng R, Lin J, Wang PC, Zhu C, Wu Y. Effect of adhesive characteristics on static strength of adhesive-bonded aluminum alloys. Int J Adhes Adhes 2015;57:85–94.
[3] Pereira AM, Ferreira JM, Antunes FV, Bártolo PJ. Analysis of manufacturing parameters on the shear strength of aluminum adhesive single-lap joints. J Mater Process Technol 2010;210:610–7.
[4] Bhowmik S, Bonin HW, Bui VT, Weir RD. Durability of adhesive bonding of titanium in radiation and aerospace environments. Int J Adhes Adhes 2006;26:400–5.
[5] Fay PA, Maddison A. Durability of adhesively bonded steel under salts pray and hydrothermal stress conditions. Int J Adhes Adhes 1990;10:179–86.
[6] Baldan A. Review: adhesively-bonded joints in metallic alloys, polymers and composite materials: mechanical and environmental durability performance. J Mater Sci 2004;39:4729–97.
[7] LaPlante G, Ouriadov AV, Lee-Sullivan P, Balcom BJ. Anomalous moisture diffusion in an epoxy adhesive detected by magnetic resonance imaging. J Appl Polym Sci 2008;109:1350–9.
[8] Wahab MA, Ashcroft IA, Crocombe AD, Shaw SJ. Diffusion of moisture in adhesively bonded joints. J Adhes 2001;77:43–80.
[9] Underhill PR, DuQuesnay DL. The role of corrosion/oxidation in the failure of aluminum adhesive joints under hot, wet conditions. Int J Adhes Adhes 2006;26:88–93.

[10] Lunder O, Olsen B, Nisancioglu K. Pre-treatment of AA6060 aluminum alloy for adhesive bonding. Int J Adhes Adhes 2002;22:143−50.
[11] Wang M, Liu A, Liu Z, Wang PC. Effect of hot humid environmental exposure on fatigue crack growth of adhesive-bonded aluminum A356 joints. Int J Adhes Adhes 2013;40:1−10.
[12] Zhang F, Wang HP, Hicks C, Yang X, Carlson BE, Zhou Q. Experimental study of initial strengths and hygrothermal degradation of adhesive joints between thin aluminum and steel substrates. Int J Adhes Adhes 2013;43:14−25.
[13] Zvetkov VL. Comparative DSC kinetics of the reaction of DGEBA with aromatic diamines. I. Non-isothermal kinetic study of the reaction of DGEBA with m-phenylene diamine. Polymer 2001;42:6687−97.
[14] Sun J, Pantoya ML, Simon SL. Dependence of size and size distribution on reactivity of aluminum nanoparticles in reactions with oxygen and MoO_3. Thermochim Acta 2006;444:117−27.
[15] TA Instruments DSC Q100. Differential scanning calorimeter-Q series™ getting started guide. American: TA Instruments; 2007.
[16] Baldan A. Adhesion phenomena in bonded joints. Int J Adhes Adhes 2012;38:95−116.
[17] Dataphysics OCA-20 contact Angle analyzer. DataPhysics products for surface chemistry. Germany: DataPhysics Instruments GmbH Company; 2003.
[18] van Oss CJ, Good RJ, Chaudhury MK. Additive and nonadditive surface tension components and the interpretation of contact angles. Langmuir 1988;4:884−91.
[19] Young T. Phil Trans R Soc Lond 1805;95:65−87. http://dx.doi.org/10.1098/rstl.1805.0005.
[20] Owens DK, Wendt RC. Estimation of the surface free energy of polymers. J Appl Polym Sci 1969;13:1741−7.
[21] Fowkes FM. Attractive forces at interfaces. Ind Eng Chem 1964;56:40−52.
[22] Mittal KL. Adhesion measurement of films and coatings. Utrecht, The Netherlands: VSP; 1995.
[23] ASTM D1002-2001. Standard test method for apparent shear strength of single-lap-joint adhesively bonded metal specimens by tension loading (metal-to-metal). American Society for Testing Materials; 2001.
[24] Liang WJ, Rometsch PA, Cao LF, Birbilis N. General aspects related to the corrosion of 6xxx series aluminum alloys: exploring the influence of Mg/Si ratio and Cu. Corros Sci 2013;76:119−28.
[25] Liu Z, Sun R, Mao Z, Wang PC. Effects of phosphate pretreatment and hot-humid environmental exposure on static strength of adhesive-bonded magnesium AZ31 sheets. Surf Coat Technol 2012;206:3517−25.
[26] Pukánszky B, Fekete E. Adhesion and surface modification. Adv Polym Sci 1999;139:109−53.
[27] Awaja F, Gilbert M, Kelly G, Fox B, Pigram PJ. Adhesion of polymers. Prog Polym Sci 2009;34:948−68.
[28] Bowditch MR. The durability of adhesive joints in the presence of water. Int J Adhes Adhes 1996;16:73−9.
[29] Zhou J, Lucas JP. Hygrothermal effects of epoxy resin part I: the nature of water in epoxy. Polymer 1999;40:5505−12.
[30] Zanni-Deffarges MP, Shanahan MER. Diffusion of water into an epoxy adhesive: comparison between bulk behavior and adhesive joints. Int J Adhes Adhes 1995;15:137−42.
[31] Vera R, Delgado D, Rosales BM. Effect of atmospheric pollutants on the corrosion of high power electrical conductors: part 1. Aluminum and AA6201 alloy. Corros Sci 2006;48:2882−900.
[32] Desiraju GR. Chemistry beyond the molecule. Nature 2001;412:397−400.
[33] Elitzur S, Rosenband V, Gany A. Study of hydrogen production and storage based on aluminum water reaction. Int J Hydrogen Energy 2014;39:6328−34.